

# Oxidation mechanisms in Si-Al-O-N ceramics

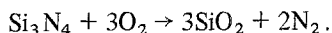
M. H. LEWIS, P. BARNARD

*Department of Physics, University of Warwick, Coventry, UK*

Oxidation mechanisms in single- and two-phase Si-Al-O-N ceramics have been studied using scanning and transmission electron microscopy together with energy-dispersive X-ray microanalysis. Silicate layers formed on single-phase ( $\beta'$ ) ceramics are non-crystalline, with viscosity and resulting oxidation kinetics controlled by outward diffusion of grain-boundary segregated impurities. Aluminium substitution in  $\beta'$  is important in compensating for the viscosity reduction imposed by the divalent ion impurities and inhibiting crystallization. Crystallization, induced only on slow furnace cooling, produces mullite and cristobalite phases. Two-phase ( $\beta'$  and matrix) ceramics exhibit comparatively poor oxidation kinetics with formation of a porous crystalline silicate layer due to the continued availability of a high concentration of metallic ions in the matrix phase.

## 1. Introduction

The successful application of  $\text{Si}_3\text{N}_4$  and related Si-Al-O-N ceramics in a high-temperature oxidizing environment is dependent on the formation of a surface oxide film via a reaction of the type:



Studies of film composition and structure, for  $\beta$ - $\text{Si}_3\text{N}_4$  ceramics have shown [1-3] that the film is a "silicate" containing a large concentration of ions derived from the impurity sintering "catalysts" (e.g. MgO) together with accidental impurities. The films are sometimes partially crystalline, containing phases such as enstatite ( $\text{MgSiO}_3$ ) in MgO-additive materials.

Recently, it has been demonstrated [4] that the "protection" conferred by the oxide film is not due to the requirement for diffusion of the components of the oxidation reaction through the film, as normally interpreted from parabolic oxidation kinetics. Rather, the oxidation rate is limited by the rate of outward diffusion of metallic impurity ions into the  $\text{SiO}_2$  film, reducing its viscosity and hence its solubility for  $\text{Si}_3\text{N}_4$ . Si is transported through the silicate layer for reaction with atmospheric oxygen. While the exact oxidation mechanism is not proven experimentally, it has been shown that outward impurity diffusion is rate-limiting by demonstrating no increase in kinetics of further oxidation on removal of the initial silicate film.

The research described in this paper was aimed at an understanding of the oxidation mechanisms in microstructurally well-characterized Si-Al-O-N ceramics, both as single-phase "hot-pressed" materials and as two-phase materials prepared by pressureless sintering.

## 2. Experimental techniques

Both hot-pressed and sintered ceramics were prepared at the Lucas Group Laboratories. Preparation techniques and the evolution of microstructure in these materials have been described previously by Lewis *et al.* [5, 6]. Hot-pressed materials are essentially single-phase  $\beta'$  of composition  $\text{Si}_5\text{AlON}_7$  with grain size  $\sim 1\ \mu\text{m}$ , containing impurity segregation at grain-boundaries (mainly Mg and Ca, within a multilayer oxygen-rich film, or Mn + Mg + Ca, depending on the presence of sintering aids MgO and  $\text{Mn}_3\text{O}_4$ ). The selected sintered material contained a large  $\text{Y}_2\text{O}_3$  additive in the form of a second-phase "yttrio-garnet"  $3\text{Y}_2\text{O}_3 \cdot 5\text{Al}_2\text{O}_3$  (with some Si-for-Al substitution) as a semi-continuous matrix for  $\beta'$  crystals (see Fig. 5).

Test sections, 6 mm  $\times$  1 mm  $\times$  3 mm were cut from bulk pressings with a high-speed diamond saw which produced an optically polished surface suitable for oxidation experiments. Oxidation was conducted in a static (air) atmosphere in an open  $\text{Al}_2\text{O}_3$  tube furnace at 1200 to 1450°C, whilst specimens were supported by high-purity platinum mesh avoiding contact with the primary (6 mm  $\times$

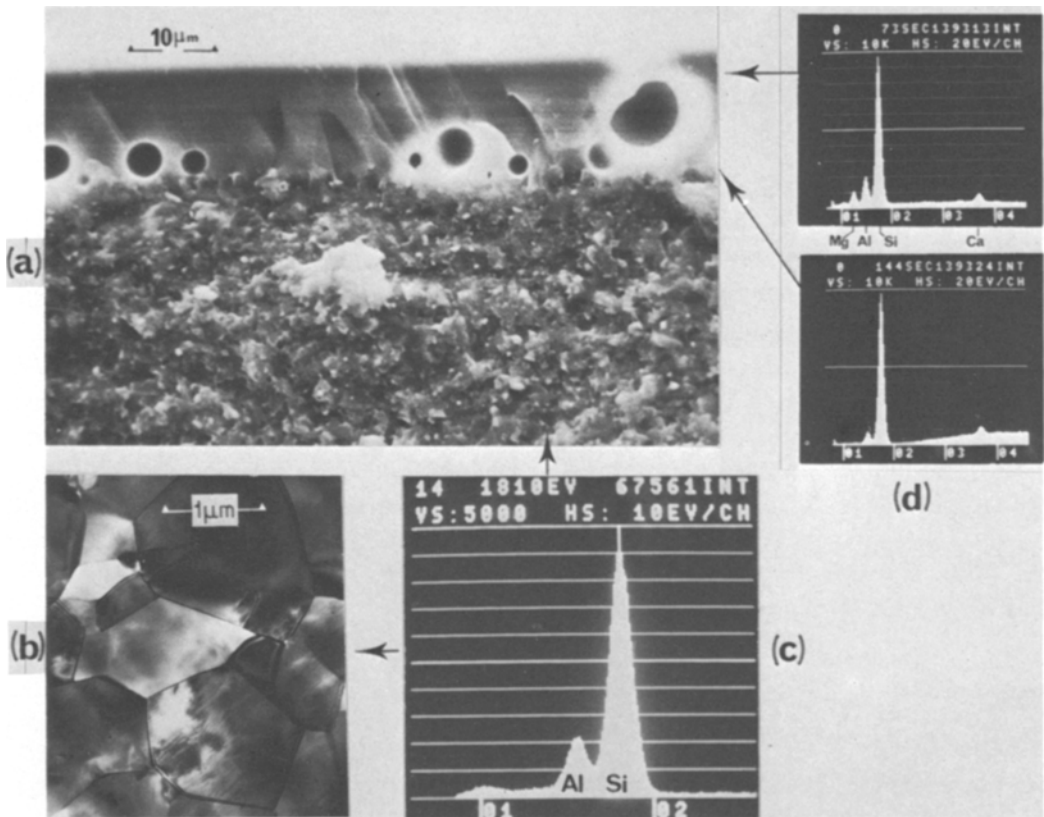


Figure 1 (a) Scanning electron micrograph (SEM) of a section through a non-crystalline silicate layer on an oxidized single-phase (Mg-containing) ceramic. The transmission electron micrograph (TEM) illustrates the typical  $\beta'$  grain structure (b) which produced the X-ray microanalysis spectrum shown in (c). In (d) the spectra show differences in segregated impurity (Mg) level through the silicate layer. (Vertical scales in the X-ray spectra are 5000 and 10000 counts in (c) and (d) respectively.)

3 mm) oxidation surfaces. Oxidation kinetics were determined from direct measurements of film thickness on specimens sectioned by transverse fracture. This technique provided clean, approximately plane, fracture surfaces for study of transverse oxide film structure and determination of chemical composition in a scanning electron microscope (SEM) fitted with an energy-dispersive X-ray analyser (EDAX).

Additional X-ray micro-analysis together with identification of crystal structure by diffraction was carried out in a transmission electron microscope fitted with SEM and scanning transmission (STEM) attachments.

### 3. Experimental observations and discussion

#### 3.1. Single-phase Si–Al–O–N ceramics

A determination of oxide film composition together with oxidation kinetics has shown that

the detrimental effect of segregated metallic impurities in single-phase Si–Al–O–N ceramics results from their outward diffusion along grain-boundaries into the  $\text{SiO}_2$  layer. Fig. 1 shows a cross-section of the oxide film in the glassy state with X-ray spectra recorded from the indicated positions. Fig. 2a summarizes the diffusional mechanisms and oxidation reaction for a Mg-containing ceramic of  $\beta'$  crystal composition  $\text{Si}_5\text{AlON}_7$ .

The outer layer of film, formed at the start of oxidation, contains the highest impurity concentration because of a progressive depletion of impurities on grain-boundaries near to the surface. Fig. 2b illustrates this depletion effect for two successive positions of the  $\beta'$ -silicate oxidation front. Grain-boundary impurity concentrations beneath the oxidation front cannot be directly measured (this would require high-resolution Auger electron spectroscopy of the intergranular

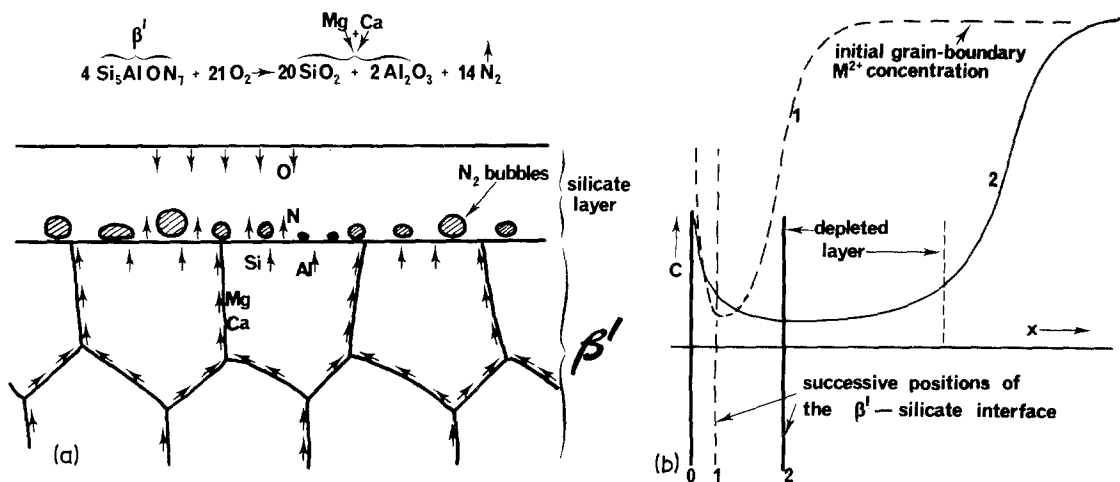


Figure 2 (a) Diagram illustrating the mechanism for oxidation which is rate-controlled by outward diffusion of grain-boundary segregated impurities. The oxidation reaction in Si–Al–O–N ceramics forms an alumino-silicate liquid with evolution of  $\text{N}_2$  gas (visible in Fig. 1a). (b) Diagram illustrating the expected concentration profiles for impurities within the silicate layer and on grain boundaries for successive positions of oxidation front.

fracture surfaces) but the rapid reduction in Mg concentration in the  $\text{SiO}_2$  film is sufficient evidence for this effect. A similar reduction occurs in the Mn impurity level in  $\text{Mn}_3\text{O}_4$ -doped ceramics and, to a lesser extent, in Ca accidental impurity levels. Al also exhibits a concentration reduction with inward movement of the oxidation front but appears in relatively high concentration (in view of its presence in  $\beta'$  crystals) via a reaction of the type illustrated in Fig. 2a. The gaseous  $\text{N}_2$  product of oxidation may initially diffuse to the surface but with increased film thickness nucleates gas bubbles near the oxidation front. At intermediate film thicknesses these bubbles expand and burst, resulting in uneven surface topography in cooled specimens. This process is aided by the reduced viscosity in the initially formed film which contains the highest Mg or Mn concentration.

A consequence of the grain-boundary depletion layer on oxidation kinetics is illustrated in Fig. 3. The lower curves represent the film thickness–time relation for the two single-phase Si–Al–O–N ceramics for a  $1350^\circ\text{C}$  temperature. These are approximately parabolic, although the experimental scatter in thickness measurement for the initial bubble-containing films is large. The re-oxidation experiment, after removal of the oxide film, demonstrates the rate-determining effect of impurities, similar to  $\beta'$ - $\text{Si}_3\text{N}_4$  ceramics [4]. The rate-limiting mechanism for oxidation is not necessarily the effect of impurity ions on solubility of the crystal components Si and N [4] but may

be the increase in inward diffusion rate of oxygen through the reduced-viscosity layer.

Oxidized specimens were normally examined in the rapidly cooled condition in an attempt to retain the structure of the film characteristic of the oxidation temperature ( $1200$  to  $1450^\circ\text{C}$ ). In all cases the silicate films showed no evidence for crystallization (this was confirmed by examining fragmented films by electron diffraction) and are believed to be high-viscosity silicate liquids during oxidation. A possible secondary effect of injection of metallic impurities into the  $\text{SiO}_2$  layer from grain-boundaries is of increasing its susceptibility to crystallization via reduced viscosity and a composition change towards, for example,  $\text{MgSiO}_3$ . Hence the stability of the liquid films in Si–Al–O–N ceramics is aided by, (i) the availability of Al from  $\beta'$  crystals, which being an intermediate ion in silicates, compensates for the viscosity-reducing tendency of Mg, Mn or Ca ions; (ii) a change of film composition such that the more sluggish mullite crystallization is more probable. This is supported by the observation of partial crystallization of these films only on very slow programmed furnace-cooling. The products of crystallization (Fig. 4) are mullite,  $\sim 3\text{Al}_2\text{O}_3 \cdot 2\text{SiO}_2$  cristobalite ( $\text{SiO}_2$ ) and an impurity-rich glassy residue. Individual crystals are large enough for X-ray micro-analysis *in situ* or by electron diffraction and micro-analysis of fragmented and dispersed films. This is the expected behaviour of an alumino-silicate with Al/Si ratio observed in

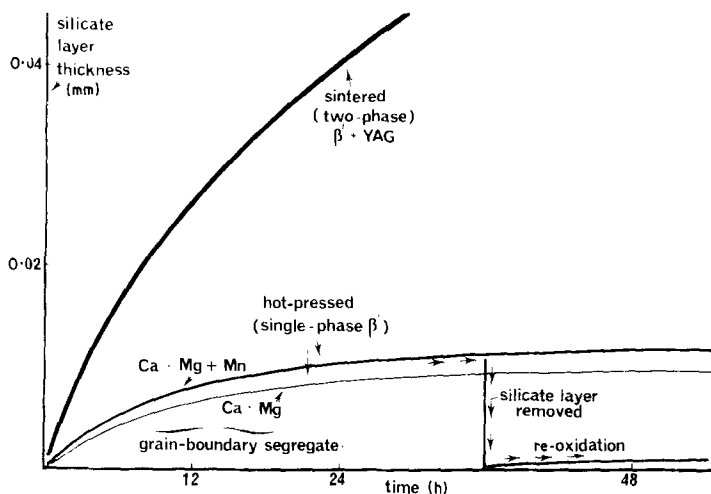


Figure 3 Comparison of approximate oxidation kinetics for single- and two-phase ceramics at 1350°C. The effect of grain-boundary impurity depletion on re-oxidation kinetics is shown for one of the single-phase ceramics.

the outer layer (Fig. 1a) and consistent with the oxidation reaction for  $\beta'$  of this substitution level (Fig. 2a). McDowell and Beall [7] have shown that such compositions are susceptible (at 1200 to 1400°C) to phase separation into  $\text{SiO}_2$ -rich globules in an  $\text{Al}_2\text{O}_3$ -rich matrix which subsequently crystallize as cristobalite and mullite.

The slow crystallization behaviour is probably not the major factor for improvement in oxidation resistance of Si-Al-O-N ceramics over silicon nitrides [8]. It has been tentatively suggested that the superiority arises from a more protective mullite film [9], but the observations made here show that long heat-treatments or slow-cooling in the 1150 to 1250°C temperature interval are necessary for crystallization. The most important factor is the maintenance of relatively high viscosity via solution of  $\text{Al}^{3+}$  ions in the silicate which

compensate for the outward diffusion of  $\text{Mg}^{2+}$  etc. impurity ions.

### 3.2. Sintered (two-phase) ceramics

The above description of single-phase oxidation leads to an immediate understanding of the relatively poor oxidation behaviour of sintered Si-Al-O-N ceramics in terms of the availability of metallic ions at the oxidation front. Fig. 3 summarizes the kinetics of silicate film growth at 1350°C on a  $\beta' + \text{yttrium aluminium garnet}$  (YAG) ceramic [6] which should be compared with the curves for single-phase ceramics at the same temperature. Fig. 5c summarizes the oxide film structure observed for various temperatures of oxidation and cooling rates. It is believed that the silicate films crystallize soon after their formation as a viscous liquid layer. The initial (now glassy) film exists in the non-crystalline, non-porous, state only near to the oxidation front (Fig. 5a and c). It contains a high level of yttrium, aluminium and impurity metallic ions which are derived from the approximately constant "reservoir" of the second (matrix) phase surrounding  $\beta'$  grains (Fig. 5b and c). It therefore crystallizes rapidly to form yttrium aluminium silicate (of undetermined structure) tridymite ( $\text{SiO}_2$ ) and a residual glass. Either the volume change on transformation, or intercrystalline fracture, induced by the  $\text{N}_2$  gas pressure, results in a porous oxide layer (Fig. 5a and c) and a degradation in the protective efficiency. The films have been shown to be porous by injecting tungsten oxide vapour into the oxidation furnace immediately before rapid cooling and detecting the tungsten X-ray

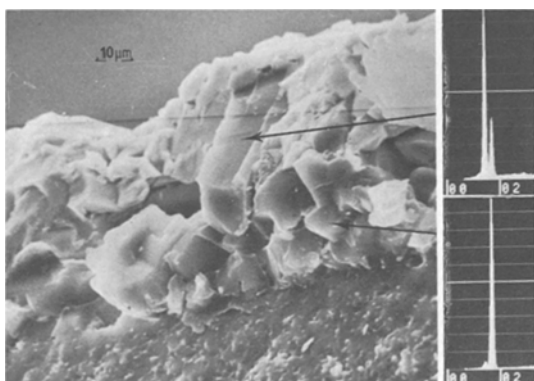


Figure 4 SEM of crystallized silicate layer formed on very slow cooling from 1400°C. Microanalysis shows the two-phase mullite and cristobalite coarse microstructure via Al and Si X-ray spectra. (Vertical scale 5000 counts.)

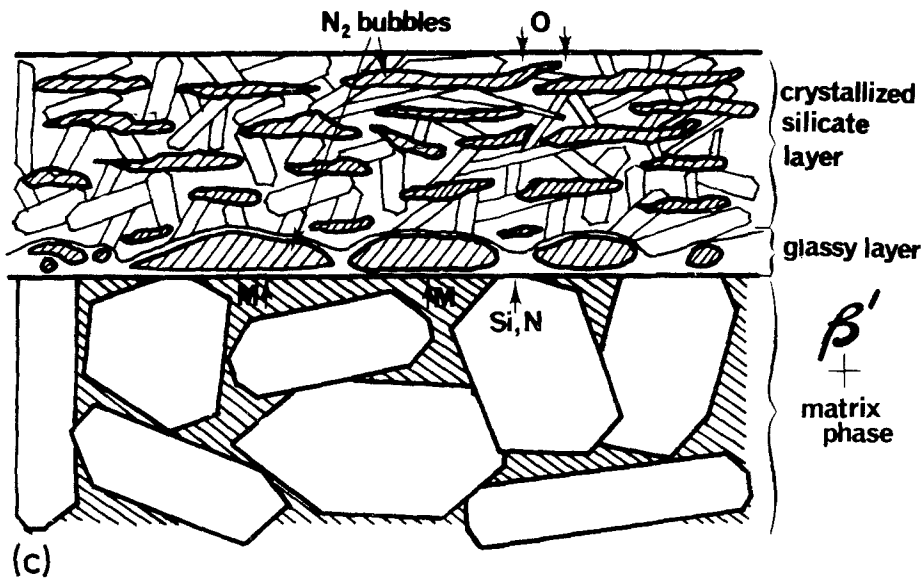
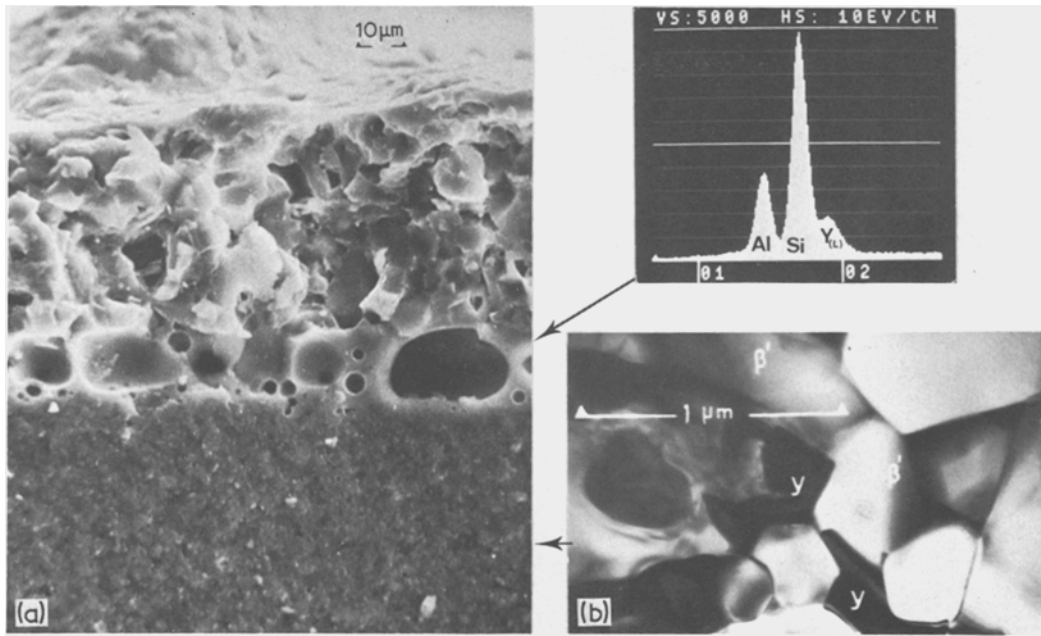


Figure 5 (a) SEM of crystalline and glassy silicate layers (containing aluminium and yttrium shown in the X-ray spectrum, with vertical scale 5000 counts) on an oxidized ( $\beta'$  and yttrio-garnet) two-phase ceramic (a TEM of this structure is shown in (b)). The “two-tier” oxide layer structure containing open porosity in the crystallized zone is sketched in (c).

emission throughout the crystallized layer cross-section of Fig. 5a.

For sintered ceramics the continued presence of a large concentration of metallic ions in the silicate layer results in a time-dependent crystallization which propagates inwards from the gas/solid interface at the oxidation temperature. The relatively thin glassy layer at the oxidation front

(Fig. 5) is not always visible on sectioned specimens.

The two factors described above, i.e. a lack of the stabilizing influence of an impurity denuded zone and formation of a porous crystalline film, may present one of the most serious limitations to engineering application of the sintered materials at elevated temperatures.

#### 4. Influence of oxidation on plasticity and fracture

An important influence of surface oxidation on creep and fracture of Si–Al–O–N ceramics at high-temperatures is anticipated for two main reasons.

(i) The most “active” centres for oxidation will be at grain-boundary/surface intersections in single-phase ceramics and the second-phase network in sintered ceramics. At these positions, intrusions of oxide film may result in stress concentrations and hence nuclei for sub-critical crack growth. (The reverse effect of “filling” of existing cracks by the silicate, thus removing stress concentrations, has been argued by some authors to account for an atmosphere/mechanical property relation. Since the film is a viscous liquid it is unlikely to be effective by this direct mechanism. An alternative explanation is that in (ii).)

(ii) The removal of metallic ions from grain-boundary segregated sites to the SiO<sub>2</sub> film in single-phase ceramics may increase intergranular cohesion and reduce diffusion rates for Si, N etc. and hence influence fracture mechanisms or diffusional deformation rates.

Recent experiments in this laboratory [10] have indicated that mechanism (ii) may be extremely important. Creep experiments in oxidizing environments have shown a time-dependent activation energy ( $Q$ ) and an apparent change in stress exponent ( $n$ ) with time in the creep equation:

$$\text{Creep rate } (\dot{\epsilon}) = A\sigma^n \exp\left(-\frac{Q}{kT}\right).$$

After long times the creep becomes steady state with  $n = 1$  and  $Q = 200 \text{ kcal mol}^{-1}$  (initially 80). This behaviour has been successfully interpreted as a purely diffusional (Coble) creep deformation

in which mass-transport occurs along grain boundaries at a rate which varies with their Mg/Ca segregate concentration. The possibility of a “non-equilibrium” impurity segregation effect between  $\beta'$  and grain-boundary, rather than oxidation, is an alternative explanation and is being studied at present.

The grain-boundary segregate type and concentration (and hence the cohesive energy of grain boundaries) also has a marked influence on the stress intensity ( $K_1$ )–crack velocity ( $V$ ) relationship for single-phase ceramics [10]. This is particularly true in the low  $K_1$ –low  $V$  regime and can have a marked effect on failure lifetimes under typical engineering service conditions.

#### References

1. A. J. KIEHLE, L. K. HEUNG, P. J. GIELISSE and T. J. ROCKETT, *J. Amer. Ceram. Soc.* **58** (1975) 17.
2. S. C. SINGHAL, *J. Mater. Sci.* **11** (1976) 500.
3. W. C. TRIPP and H. C. GRAHAM, *J. Amer. Ceram. Soc.* **59** (1976) 399.
4. D. CUBICCIOTTI, K. H. LAU and R. L. JONES, *J. Electrochem. Soc.* December (1977) 1955.
5. M. H. LEWIS, B. D. POWELL, P. DREW, R. J. LUMBY, N. NORTH and A. J. TAYLOR, *J. Mater. Sci.* **12** (1977) 61.
6. M. H. LEWIS, A. R. BHATTI, R. J. LUMBY and B. NORTH, *ibid.* **15** (1980) 438.
7. J. F. MACDOWELL and G. H. BEALL, *J. Amer. Ceram. Soc.* **52** (1969) 17.
8. W. J. ARROL, in “Ceramics for High-Performance Applications”, Proceedings of the Second Army Materials Technology Conference, Hyannis, November 1973 (Brook Hill, Mass., 1974) p. 729.
9. K. H. JACK, *J. Mater. Sci.* **11** (1976) 1135.
10. B. S. B. KARUNARATNE and M. H. LEWIS, *ibid.* **15** (1980) 449.

Received 10 May and accepted 16 July 1979.